minerals

MDPI

Article

Thermodynamic Analysis of Mineral Phase Composition of Steel Slag System

Shuai Hao, Guoping Luo *, Yuanyuan Lu, Shengli An, Yifan Chai and Wei Song

School of Materials and Metallurgy, Inner Mongolia University of Science and Technology, Baotou 014010, China
* Correspondence: luoguoping3@126.com

Abstract: In order to transform the crystalline form of Ca_2SiO4 (C_2S) in phosphorus-containing slag from monoclinic β-polycrystalline to square γ-polycrystalline, a volume expansion of about 11% was generated, which caused the phosphorus-containing slag to undergo self-powdering. The CaO-SiO_2-Al_2O_3-MgO-MnO-P_2O_5-FeO slag system was analyzed using FactSage7.1 thermodynamic software, and the effects of different P_2O_5, FeO and basicity on the mineral phase composition of slag system were analyzed in the range of 1300~1700 °C. It was shown that P_2O_5, FeO and basicity all have an effect on the composition of the mineral phases. When the mass fraction of P_2O_5 in the slag was lower than 0.25%, it had less effect on the transformation of C_2S crystalline structure. When the P_2O_5 content was higher than 0.25%, it was favorable to the generation of low-melting-point substances, but the P_2O_5 in the slag reacted with C_2S in the silicate phase, making P^{5+} solidly soluble in C_2S, inhibiting the transformation of β-C_2S to γ-C_2S and hindering the self-powdering of the slag. The FeO content in the slag system ranged from 20% to 28%, and as the FeO content increased, the C_2S content in the silicate phase decreased from 33.3% to 25.9%, while the temperature at which the silicate was completely dissolved into the liquid phase decreased from 1600 °C to 1500 °C and the complete melting temperature of the slag decreased. The low FeO content facilitates the self-powdering of slag. In the high-phosphorus slag, at temperatures below 1450 °C, with the increase of basicity, the proportion of C_2S in the silicate phase first increased and then decreased. With basicity at 1.8; the highest content of silicate phase, accounting for 33.7%; and the temperature exceeding 1450 °C, the silicate phase dissolved into the liquid phase, which is conducive to the removal of phosphorus from the slag, achieving the self-powdering of high-phosphorus slag.

Keywords: slag; mineral phase composition; self-powdering; dephosphorization

check for updates

Citation: Hao, S.; Luo, G.; Lu, Y.; An, S.; Chai, Y.; Song, W. Thermodynamic Analysis of Mineral Phase Composition of Steel Slag System. *Minerals* **2023**, *13*, 643. https://doi.org/10.3390/min13050643

Academic Editors: Daniela Guglietta, Stefano Milia, Giovanna Cappai and Adalgisa Scotti

Received: 6 March 2023
Revised: 29 April 2023
Accepted: 3 May 2023
Published: 6 May 2023

Copyright: © 2023 by the authors. Licensee MDPI, Basel, Switzerland. This article is an open access article distributed under the terms and conditions of the Creative Commons Attribution (CC BY) license (https://creativecommons.org/licenses/by/4.0/).

1. Introduction

Iron and steel metallurgy is the process of reducing and refining iron ore or scrap steel into ingots or continuous casting billets, and the smelting process generates a large amount of solid waste [1]. Converter steel slag is a solid waste produced during the steelmaking process in the converter [2]. Steel slag has the following characteristics: high yield, complex composition, poor bulk stability, high density (3.1–3.6 g/cm^3), good wear resistance (wear index of 0.7) and good compressibility (crushing value of 20.4%–30.8%) [3]. Steel slag, with the lowest utilization rate of the steel industry, is the solid waste that is most difficult to deal with. It has been of great interest to the majority of researchers and scholars. The physical properties and mineral phase composition of hot steel slag depend on its chemical composition and cooling method. In the steelmaking process, the slag is formed from the melting of the charge until the steel is discharged [4]. The steelmaking process involves melting the furnace charge at high temperatures to form a liquid state, i.e., steel and other impurities. Impurities, i.e., slag, mainly include: oxides and sulfides from the oxidation of the furnace charge, eroded furnace lining and furnace charge, precipitates in the metal charge and other impurities. Steel slag mainly comes from the converter blowing oxygen-smelting process of oxidation of Si, Mn, Fe, P and other elements in the iron; the formation

of FeO, P_2O_5 and SiO_2 primary slag; and the reaction with the addition of alkaline slagging materials combined to produce low-melting-point mineral phase. Therefore, there are many silicate minerals in steel slag, whose chemical composition is similar to that of silicate cement clinker. According to the different processes used, steel slag can be divided into converter slag, electric furnace slag, refining slag, casting residue slag and iron pretreatment slag [5], water-quenched steel slag, lump steel slag and powder steel slag. Slag-making materials are added in different amounts, resulting in different alkalinity levels of steel slag, which can be divided into: low-alkalinity steel slag (R_2 = 1.3~1.8), medium-alkalinity steel slag (R_2 = 1.8~2.5) and high-alkalinity steel slag (R_2 > 2.5).

According to the information of the Bureau of Statistics, the output of crude steel reached 1.03 billion tons in 2021, and the output of steel slag was about 130 million tons, accounting for about 12%~15% of the output of crude steel. The cumulative stock of steel slag has exceeded 800 million tons, of which about 80% is converter steel slag [6]. Steel slag, as a major industrial solid waste, has a chemical composition and mineral composition very similar to that of cement and concrete raw materials. However, the low content of cementitious active substances in steel slag, its poor stability and high crushing cost have become the main factors limiting the scale and resource utilization of steel slag in cement admixtures and construction. If the steel slag can achieve self-powdering during the cooling process, it will reduce the cost of steel slag crushing. However, so far, most steel mills still treat converter slag with traditional methods, such as piling and landfilling, and its recovery rate is only about 30%, which not only brings huge environmental pressure, but also causes a huge waste of resources and greatly increases the cost of steelmaking [7]. It was found that phosphorus in converter slag is highly enriched with C_2S in steel slag to form C_2S-C_3S, which has a large impact on the self-powdering of steel slag [8,9]. The higher P_2O_5 content inhibited the conversion of β-C_2S to γ-C_2S and hindered the self-powdering of steel slag. The transformation of β-C_2S to γ-C_2S in the slag produces a volume expansion of about 11%, allowing the slag to undergo self-powdering [10–12]. Chuan-ming Du et al. [13] investigated the effect of Fe^{2+} (Fe^{2+}/T.Fe) content on the leaching solid solution of P_2O_5 using the leaching of concentrated phosphorous solid solution from steel slag. It was found that the increase in the proportion of Fe^{2+} (Fe^{2+}/T.Fe) in the slag decreased the P_2O_5 content in the solid solution and increased the solid solution mass. Therefore, it is believed that with the increase of Fe^{2+} ratio in steel slag, most P is still distributed in the solid solution. The temperature and basicity of the slag have a great influence on the composition of the mineral phase in the slag, which varies at different temperatures and basicity [14]. The simulation of experiments using FactSage7.1 thermodynamic calculation software [15], GTT-Technologies, Herzogenrath, Germany) to analyze the variation pattern of C_2S in the silicate phase is essential for the study of slag self-powdering [16].

In this paper, the CaO-SiO_2-Al_2O_3-MgO-MnO-P_2O_5-FeO slag system was studied and the effect of slag temperature (1300–1700 °C) on the mineral phase composition was analyzed using the Equilib module of FactSage7.1 thermodynamic calculation software. The influence law of P_2O_5, FeO and basicity on the mineral phase composition of the slag was systematically studied [17,18], providing a reference for the effective utilization of phosphorus-containing slag.

2. Experiments and FactSage7.1 Simulation Calculations

2.1. Slag System Allocation Scheme

In this study, the actual slag of the converter in the late stage of iron smelting in a steel plant was used as the design basis, and the pure reagent of CaO-SiO_2-Al_2O_3-MgO-MnO-P_2O_5-FeO slag system [19] was used as the raw material. Eighteen ore formulations with variable P_2O_5, FeO and basicity were designed ($R_2 = \frac{\omega(CaO)}{\omega(SiO_2)}$) as shown in Table 1.

Table 1. Slag system ore blending scheme (mass fraction, %).

Chemical Composition	*w* (CaO)	*w* (SiO_2)	*w* (Al_2O_3)	*w* (MgO)	*w* (MnO)	*w* (P_2O_5)	*w* (FeO)	Basicity
1	39.91	19.95	1.86	7.36	4.92	0.000	26	2.00
2	39.82	19.91	1.86	7.36	4.92	0.125	26	2.00
3	39.74	19.87	1.86	7.36	4.92	0.250	26	2.00
4	39.57	19.79	1.86	7.36	4.92	0.500	26	2.00
5	39.41	19.70	1.86	7.36	4.92	0.750	26	2.00
6	39.24	19.62	1.86	7.36	4.92	1.000	26	2.00
7	39.07	19.54	1.86	7.36	4.92	1.250	26	2.00
8	38.91	19.45	1.86	7.36	4.92	1.500	26	2.00
9	38.74	19.37	1.86	7.36	4.92	1.750	26	2.00
10	38.57	19.29	1.86	7.36	4.92	2.000	26	2.00
11	42.74	21.37	1.86	7.36	4.92	1.750	20	2.00
12	41.41	20.70	1.86	7.36	4.92	1.750	22	2.00
13	40.07	20.04	1.86	7.36	4.92	1.750	24	2.00
14	37.41	18.70	1.86	7.36	4.92	1.750	28	2.00
15	35.76	22.35	1.86	7.36	4.92	1.750	26	1.6
16	37.36	20.75	1.86	7.36	4.92	1.750	26	1.8
17	39.95	18.16	1.86	7.36	4.92	1.750	26	2.2
18	41.02	17.09	1.86	7.36	4.92	1.750	26	2.4

2.2. Parameters Setting of FactSage7.1

The Equilib module in FactSage7.1 was used to calculate the mineral phase composition of 100 g slag at equilibrium under different temperature conditions and to analyze the variation of its mineral phase composition. The specific parameter conditions are shown in Table 2. The thermodynamic calculation temperature range is 1300 to 1700 °C with a step size of 50 °C. The ambient pressure is set to approximately 101.325 kPa for 1 standard atmosphere.

Table 2. Parameter settings of FactSage7.1.

Database	FToxid7.1, FactPS7.1
Base-Phase	Slag, Clinopyroxene, Monoxide, Liquid, oxides, spinel, wollastonite, bC_2S, aC_2S, melilite, olivine

2.3. Validation Experiments

The raw materials were configured according to the chemical composition of 9# specimens using pure reagents. The raw materials were loaded into a ball mill jar and mixed on a ball mill (T = 2 h), and the samples were prepared using a press (pressure: 6 MPa, shape: d15 mm × h6 mm cylindrical). The specimens were placed in corundum crucibles and heated from room temperature to 1000 °C using the KTF-1700-VT high-temperature vertical furnace (KTF-1700-VT, Kemi Instrument, Nanjing, China) with a heating regime of 10 °C/min, and then from 1000 °C to 1450 °C with a heating regime of 5 °C/min and held for 1 h. The samples were removed and air-cooled to room temperature for use.

The detection method was as follows: he degree of response was assessed by photographing the specimen's apparent morphology. The tests were carried out using a D8-advanced X-ray diffractometer (Germany Brock, Groß Ippener, Germany) with the setting conditions Cu-Kα target, a scanning range of 20°~80° and a speed of 5°/min. Scanning type was as follows: emitter–detection linkage, scanning voltage of 20 kV and scanning current of 5 mA. The mixed slag mineral phase composition was analyzed using SEM-EDS (Japan Electronics, Tokyo, Japan) scanning electron microscopy to verify the accuracy of FactSage7.1 simulation calculation results.

3. Results and Discussion

3.1. Mineral Phase Composition

In order to verify the accuracy of the equilibrium mineral phase composition of the thermodynamic calculation software, the 9# roasted specimens were scanned and analyzed using a D8-advanced XRD diffractometer (Germany Brock, Groß Ippener, Germany) after grinding, and the results are shown in Figure 1. According to Figure 1, the main diffraction peaks of 9# slag are yellow feldspar crystals ($Ca_2Al_2SiO_7$) and magnesium yellow feldspar (Ca_2MgSiO_7), where $Ca_2Al_2SiO_7$ (ICSD card # 74-1607) has a diffraction angle 2θ of 31.433° and crystal plane spacing d value of 0.1756 nm; the diffraction angle 2θ of Ca_2MgSiO_7 (ICSD card # 76-0841) is 31.232° with a crystalline surface spacing d value of 0.1747 nm; the diffraction peaks were similar, and therefore it was concluded that the main mineral phases in the synthesized slag were $Ca_2Al_2SiO_7$ and Ca_2MgSiO_7. The diffraction peaks of Fe_2SiO_4, Mg_2SiO_4 and $MgAl_2O_4$ were relatively weak, the diffraction peaks of the three were similar, the diffraction peaks at diffraction angles 2θ of 44.645° and 64.980° were similar and the diffraction intensity was moderate. The diffraction peaks of $CaAl_2O_4$ with weak diffraction intensity were found at 2θ of 31.506° and 35.597°. Because of the high overlap of XRD diffraction peaks, the composition of the main mineral phases in the synthetic slag could not be determined, so SEM scanning electron microscopy was used to analyze the structure and composition of the mineral phases of specimen 9.

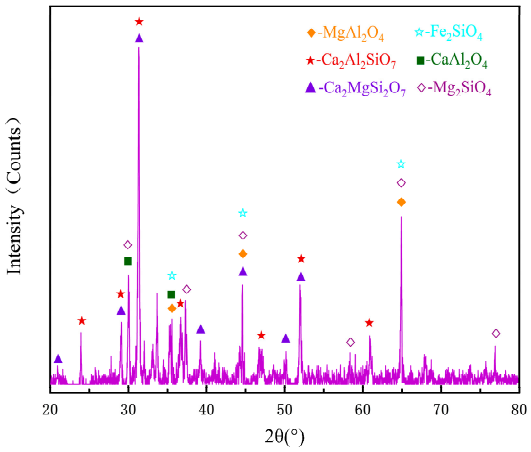


Figure 1. XRD pattern of specimen No. 9.

Figures 1 and 2 and Table 3 show the results of specimen No. 9 being warmed to 1450 °C, rapidly cooled to room temperature and examined via SEM scanning electron microscopy, and Figure 4 shows the analysis results of FactSage7.1 thermodynamic calculation software. The main chemical composition and percentage of silicates at 1450 °C in Figure 4 are: 0.537% Mg_2SiO_4, 0.283% Fe_2SiO_4, 15.234% Ca_2SiO_4 and 0.165% Mn_2SiO_4. The main chemical composition and percentage of monoxide are: 2.854% FeO, 0.157% Fe_2O_3, 0.091% CaO and 4.083% MgO. The main chemical composition and percentage of liquid phase are: 1.859% Al_2O_3, 13.694% SiO_2, 28.729% CaO, 17.618% FeO, 1.687% Fe_2O_3, 2.970% MgO, 3.139% MnO, 0.013% Mn_2O_3 and 1.750% P_2O_5. From the above data, it is clear that the temperature is mainly Ca_2SiO_4 in the silicate mineral phase, FeO, MgO and MnO in monoxide, and CaO, SiO_2 and FeO in the liquid phase.

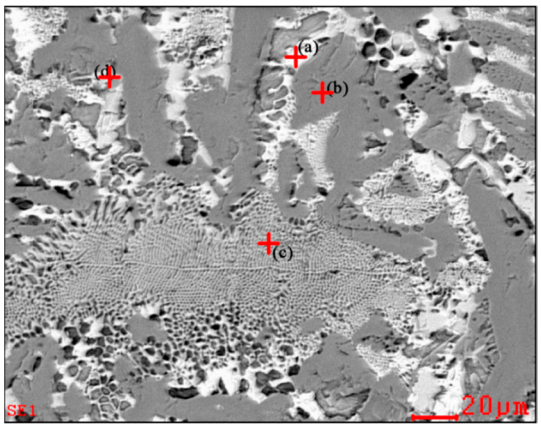


Figure 2. SEM point scanning diagram of slag (**a**–**d**).

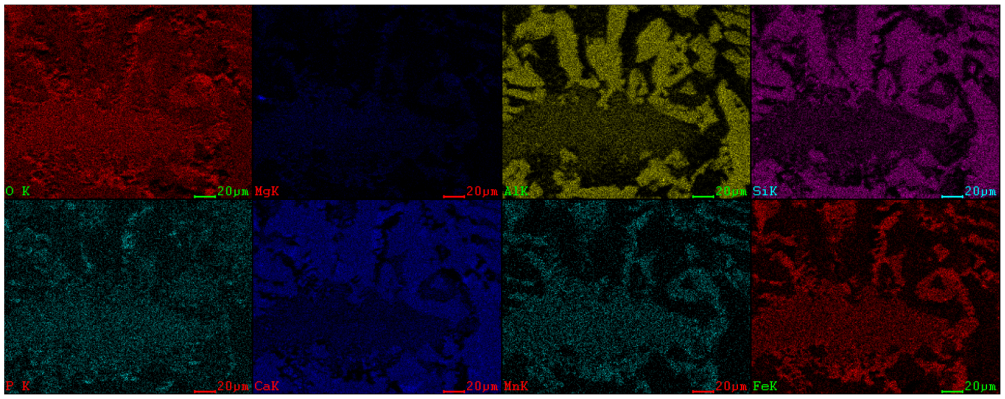


Figure 3. SEM surface scanning of slag containing P.

Table 3. EDS analysis results of each point (mass fraction, %).

Point	O	Mg	Al	Si	P	Ca	Mn	Fe
(a)	48.46	10.69	02.16	00.59	00.41	01.82	05.36	29.60
(b)	48.68	01.06	15.18	12.19	00.14	18.45	00.04	04.14
(c)	50.93	08.58	07.40	04.31	01.62	09.31	02.94	13.91
(d)	49.41	01.30	02.85	05.12	00.92	25.19	01.55	09.99

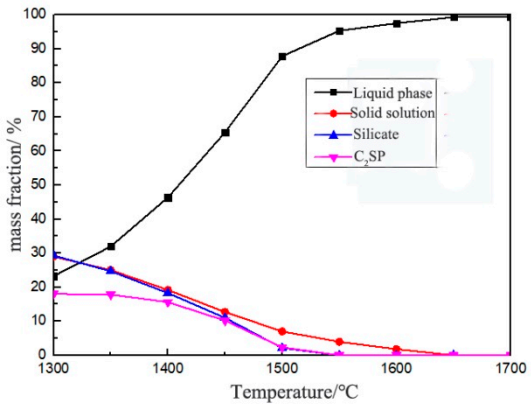


Figure 4. Mineral phase composition of slag at 1450 °C.

After scanning electron microscopy analysis, as shown in Figures 2 and 3, the main elements at a were shown to be Fe, O, Mg and Mn, which were analyzed as $MgFe_2O_4$

phase. The mineral phase did not appear in XRD, but was present as compounds such as Fe_2SiO_4, Mg_2SiO_4 and $MgAl_2O_4$. The analysis suggests that it may be that the XRD scan range is small for the scan of this mineral phase. The main elements at b were Ca, Si, Al and O. The analysis suggests that the phase is $Ca_2Al_2SiO_7$. The main elements at c were Fe, Ca, Si, Mg, Al and o, and a small amount of P element, which was considered to be solid solution phase containing phosphate, spinel and rosaceite. The P-bearing mineral phase was not found in the XRD diffraction pattern, and the analysis combined with the scanning process suggests that it was not identified during the scanning process due to its low content. The main elements at d were Ca, Si and O. The material phase at d was analyzed as silicate. In the XRD diffraction pattern, silicate mineral phases existed in the form of Fe_2SiO_4 and Mg_2SiO_4. Combined with the SEM surface scan, the main phases of the slag were analyzed as yellow feldspar crystals ($Ca_2Al_2SiO_7$), accounting for about 47.3%, rose pyroxene ($(Mn, Fe, Ca)_5(Si_5O_{15})$), accounting for about 10.7%, magnesia yellow feldspar ($Ca_2MgSi_2O_7$), accounting for about 3.4%, magnesia aluminum spinel ($MgAl_2O_4$), accounting for about 1.9%, magnesia iron spinel ($MgFe_2O_4$), accounting for about 21.2%, magnesium silicate (Mg_2SiO_4), accounting for about 2.1%, calcium phosphate ($Ca_3(PO_4)_2$), accounting for about 1.2% and dicalcium silicate (Ca_2SiO_4), accounting for about 10.6%. At a basicity of 2.0 and a temperature of 1450 °C, the solid solution percentage was found to be 12.7%, the silicate percentage was 11.0%, the a-Ca_2SiO_4-$Ca_3(PO_4)_2$ percentage was 10.1% and the liquid phase percentage was 65.5% as determined by FactSage7.1 analysis. Since SEM scans were measured at room temperature and FactSage7.1 was calculated at a temperature of 1450 °C, the experimentally obtained data were considered to be converted according to the melting point of the substance, and the conversion results were in good agreement with the calculated results. The calculated slag system was basically consistent with the actual slag system, and the calculated and analyzed mineral phase composition of allotropic minerals using FactSage7.1 had a certain degree of confidence.

3.2. Effect of P_2O_5 on Slag Mineral Phase Composition

The effects of different P_2O_5 contents on the composition of the slag phase of the CaO-SiO_2-Al_2O_3-MgO-MnO-P_2O_5-FeO slag system in the range of 1300–1700 °C are shown in Figure 5. Since the silicate phase was dominated by C_2S, which is a high-melting-point mineral phase, silicate melting was not considered at 1300 °C. When the slag did not contain P_2O_5, the temperature was 1300 °C; the silicate mineral phase was dominated by C_2S; the amount of liquid phase accounted for 23.123%; the liquid phase was dominated by magnesia-silica calcium stone ($Ca_3MgSi_2O_8$) and the binary basicity in the liquid phase was 3.1. With the increase of temperature, the content of C_2S in the mineral phase of silicate gradually decreased, the amount of liquid phase kept increasing and the binary basicity in the liquid phase kept decreasing; when the slag temperature exceeded 1550 °C, the C_2S in the mineral phase completely disappeared, and the percentage of liquid phase was 84.443%. When the temperature reached 1600 °C, the basicity in the liquid phase dropped to about 2.0, the liquid phase percentage was 96.038% and the slag melted completely to meet the design requirements. With the increase of P_2O_5 content, the amount of liquid phase tended to increase at the same temperature, and when the temperature reached 1600 °C, the slag was in a completely melted state. The silicate mass fraction decreased from 49.5% to 27.7% at a basicity of 2.0, FeO content of 26% and an increase of P_2O_5 percentage from 0% to 2%. This indicates that the increase of P_2O_5 inhibits the generation of silicate phase, and the silicate phase melts into the liquid phase when the temperature exceeded 1600 °C and when the percentage of P_2O_5 was lower than 0.5%. The silicate phase disappeared when the percentage of P_2O_5 exceeded 0.5% and the temperature exceeded 1550 °C, indicating that, as the percentage of P_2O_5 increases, it is beneficial to reduce the melting temperature of silicate [20]. When the P_2O_5 content in the slag was higher than 0.25%, $Ca_7P_2Si_2O_{16}$ ($Ca_3(PO_4)_2 + 2Ca_2SiO_4$) [21] phase appeared in the slag, and the slag temperature increased from 0.5% to 2% and $Ca_7P_2Si_2O_{16}$ content increased from 0.3% to 20.5% at 1300 °C. This indicates that P_2O_5 can react with the mineral phase in the slag to produce the $Ca_7P_2Si_2O_{16}$

reaction, and with the increase of temperature, $Ca_3(PO_4)_2 + 2Ca_2SiO_4$ begins to decompose into Ca^{2+} ion and P_2O_5, and P_2O_5 is decomposed to combine with Fe^{2+} and Mn^{2+} in solution to form Fe_2P, Mn_2P and other mineral phases [22]. When the slag temperature exceeded 1500 °C, $Ca_7P_2Si_2O_{16}$ disappeared, at which time the liquid phase accounted for 92.35% and the slag was in a completely melted state. The addition of P_2O_5 is beneficial to the generation of low-melting-point substances and can play a role in reducing the melting temperature of the slag [23]. On the other hand, considering the increase of P_2O_5 content, P_2O_5 in the slag reacts with C_2S in the silicate phase, making the solid solution of P^{5+} ions into C_2S, inhibiting the transformation of β-C_2S to γ-C_2S [24], hindering the self-powdering of the slag to proceed and increasing the production cost of the subsequent process of the slag. For the dephosphorization and subsequent treatment of high-phosphorus slag, the slag temperature should be increased to facilitate the removal of phosphorus from the slag. In summary, the content of P_2O_5 in the slag should be controlled below 0.25% and the temperature above 1500 °C, which can assist with achieving the self-powdering of the slag.

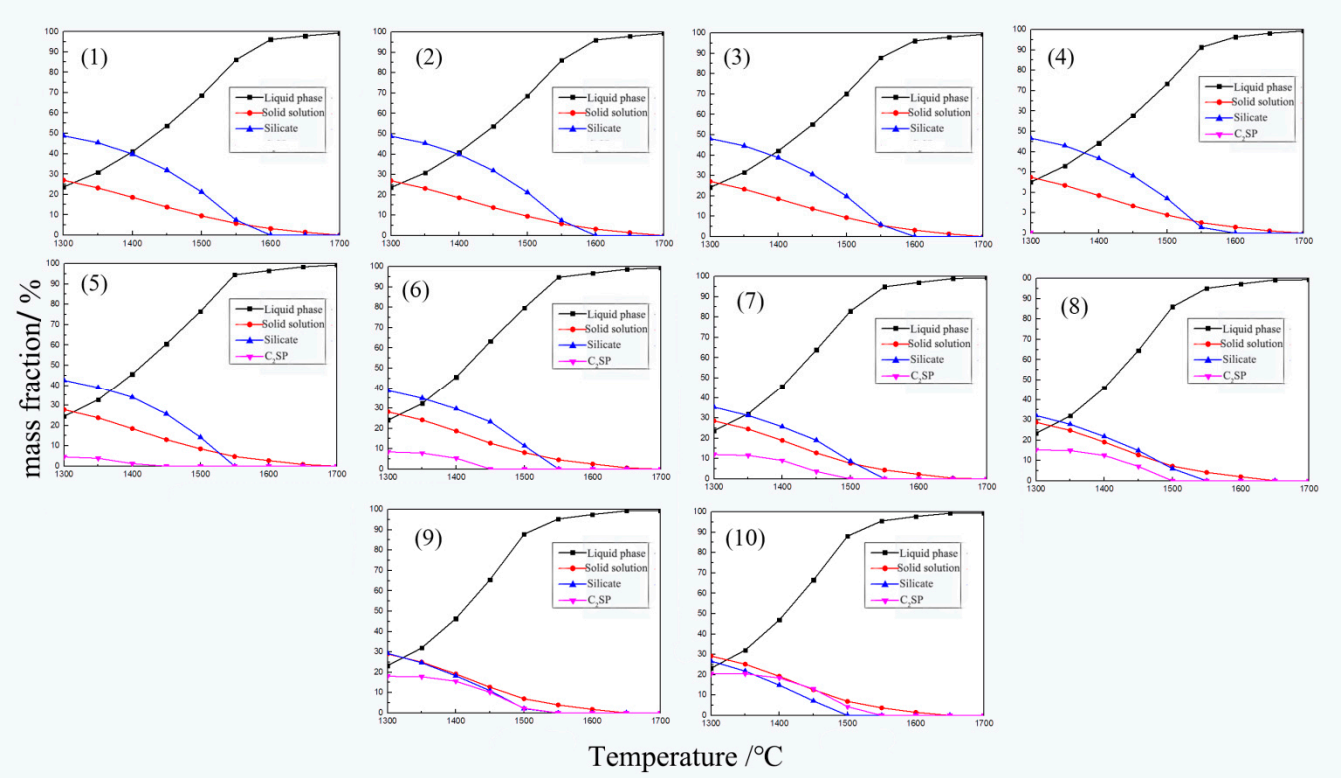


Figure 5. Influence of P_2O_5 on slag mineral phase composition ((**1**–**10**) are specimens 1~10, respectively).

3.3. Effect of FeO on the Physical Composition of Slag

The influence of FeO on the slag composition was analyzed by FactSage7.1, calculating the composition of the mineral phase of (specimens 9, 11~14) at 1300~1700 °C. When the percentage of P_2O_5 in the slag was 1.75% and the percentage of FeO was 20%–28%, the silicate phase was dominated by C_2S and $Ca_3MgSi_2O_8$, the percentage of C_2S in the silicate phase decreased as the percentage of FeO increased, the FeO was 20%, $Ca_7P_2Si_2O_{16}$ was generated in the phase at the temperature of 1300 °C, and the phase disappeared as the temperature increased. As can be seen from Figure 6, the FeO percentage increased from 20% to 28%, and the C_2S percentage in the silicate phase decreased from 33.3% to 25.9% at a temperature of 1300 °C. With the increase of FeO content, the temperature of silicate melting into the liquid phase decreased from 1600 °C to 1500 °C, and the complete melting temperature of slag also decreased with the increase of FeO. It was found that with

the increase of FeO content in the slag, the dissolution of silicate was promoted and the complete melting temperature of the slag was reduced.

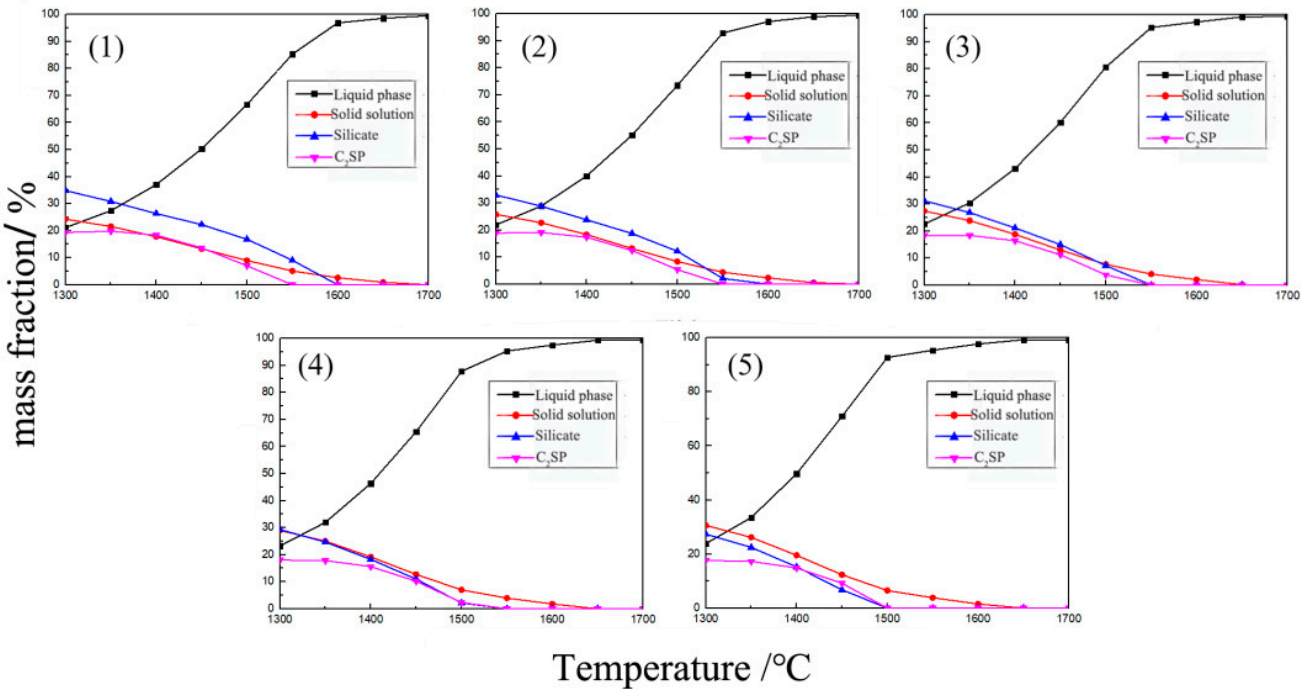


Figure 6. Effect of FeO on slag mineral phase composition. (**1**) Specimen No. 11; (**2**) Specimen No. 12; (**3**) Specimen No. 13; (**4**) Specimen No. 9; (**5**) Specimen No. 14.

3.4. Effect of Basicity on the Composition of the Slag Phase

The effect of different basicity on slag composition was analyzed by FactSage7.1 calculating the composition of the mineral phase of (specimens 9, 15~18) at 1300~1700 °C. The effect of basicity and temperature on the slag phase is shown in Figure 7. The analysis revealed that the silicate phase content tended to increase and then decrease when P_2O_5 was 1.25%, basicity increased from 1.6 to 2.4 and temperature was 1300 °C. At a basicity of 1.6 and a temperature of 1300 °C, the silicate percentage was 18.9%. When the basicity increased to 1.8, the percentage of silicate phase was the highest, 33.7%. When the basicity was higher than 1.8, the percentage of silicate phase gradually decreased with the increase of basicity, and when the basicity was 2.4, the percentage of silicate phase was only 11.6%. When the temperature exceeded 1450 °C, the silicate material phase dissolved into the liquid phase. At a basicity of 1.6 and a temperature of 1300 °C, a magnesium–silica–calcium stone ($Ca_3MgSi_2O_8$) phase was produced, and at a basicity of 1.8 and a temperature of 1300 °C, a-C_2S-C_3P solid solution was produced. With a basicity of 2.2 and a temperature of 1300 °C, a magnesium–silica–calcite $Ca_3MgSi_2O_8$, a-C_2S-C_3P solid solution was generated. At a basicity of 2.4 and a temperature of 1300 °C, $Ca_7P_2Si_2O_{16}$, $Ca_3MgSi_2O_8$, a-C_2S-C_3P solid solution was generated in the slag. When the basicity was lower than 1.6, the slag was dominated by magnesium rose pyroxene, and when the basicity was between 1.6 and 2.4, the slag was dominated by silicate phase. The reason for this is that when the basicity in the slag is low, the dephosphorization is sufficient and C_2S cannot precipitate advantageously, and as the basicity rises, the dephosphorization kinetics are insufficient and C_2S precipitates advantageously in the slag; when the basicity is 2.0~2.4, the large amount of C_2S in the slag will inhibit the generation of magnesium–silica calcium stone ($Ca_3MgSi_2O_8$), which is favorable to the generation of a-C_2S-C_3P solid solution and makes the C_2S in the material phase decrease. When the basicity was lower than 1.8, increasing the basicity was beneficial to the generation of silicate phase, and the silicate phase disappears when the slag temperature was higher than 1450 °C. When the basicity was higher than

1.8, the content of silicate phase decreased with the increase of basicity, and the silicate phase disappeared when the temperature exceeded 1450 °C. It was shown that the silicate content in the material phase increased significantly with the increase of basicity below 1.8, which shows that controlling the basicity in the range of 1.6 to 2.0 is more favorable for the self-powdering of slag.

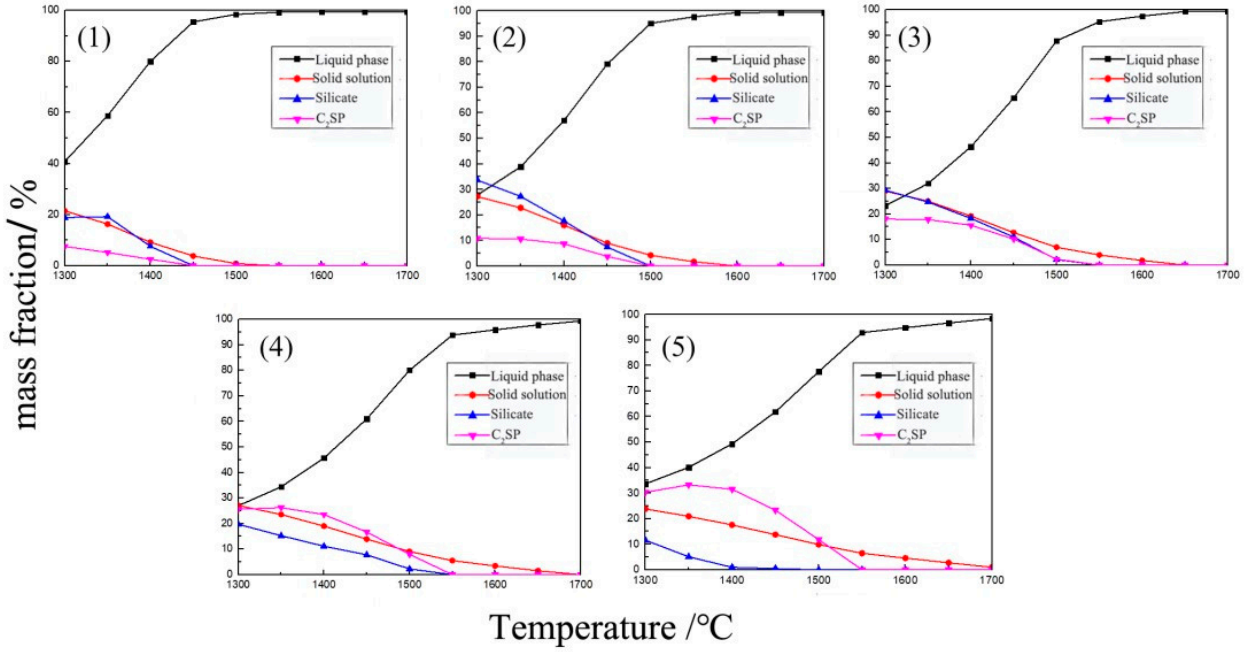


Figure 7. Influence of basicity and temperature on slag mineral phase composition. (**1**) Specimen No. 15; (**2**) Specimen No. 16; (**3**) Specimen No. 9; (**4**) Specimen No. 17; (**5**) Specimen No. 18.

4. Conclusions

(1) The effect of P_2O_5 content in steel slag and temperature on self-powdering: when the mass fraction of P_2O_5 is higher than 0.25%, P^{5+} ions are solidly soluble in Ca_2SiO_4, which inhibits the conversion of β-C_2S to γ-C_2S and inhibits the self-powdering of steel slag; the mass fraction of P_2O_5 is lower than 0.25% and the temperature is controlled above 1500 °C, which is beneficial to the self-powdering of slag.

(2) The effect of FeO mass fraction on the self-powdering of steel slag: the FeO mass fraction in steel slag is higher than 20%; with the increase of FeO content, the complete melting temperature of steel slag decreases, which promotes the dissolution of silicate and inhibits the generation of Ca_2SiO_4 in the silicate phase, which is not conducive to the self-powdering of steel slag. The FeO mass fraction below 20% is conducive to the generation of Ca_2SiO_4 in the silicate phase, which is conducive to the realization of slag self-powdering.

(3) The effect of basicity on the self-powdering of steel slag is as follows: when the basicity is between 1.6 and 2.0, the precipitation of Ca_2SiO_4 in silicate phase is promoted. When the basicity is higher than 2.0, a large amount of Ca_2SiO_4 in slag will inhibit the formation of $Ca_3MgSi_2O_8$ and promote the formation of A-C_2S-C_3P phase, which is not conducive to the realization of self-powdering of slag.

Author Contributions: S.H. provided experimental data and analysis, analyzed experimental results and wrote the paper. G.L. guided the theory of the paper and modified the relevant content of the paper. Y.L. edited the language, integrated the data and corrected the experimental data in the paper. S.A. provided financial support and experimental guidance. Y.C. and W.S. guided the whole experimental process. All authors have read and agreed to the published version of the manuscript.

Funding: The project was supported by the National Key R&D Program (2020YFC1909105); Inner Mongolia Autonomous Region Science and Technology Major Special Project (2021ZD0016) and Special Project on Carbon Neutralization Research of Higher Education Institutions in Inner Mongolia Autonomous Region (STZX202231). Basic research funds for colleges and universities.

Data Availability Statement: All authors can confirm that all data used in this article are available for publication.

Conflicts of Interest: No conflicts of interest exist in the submission of this manuscript, and the manuscript is approved by all authors for publication.

References

1. Toniolo, S.; Marson, A.; Fedele, A. Combining organizational and product life cycle perspective to explore the environmental benefits of steel slag recovery practices. *Sci. Total Environ.* **2023**, *867*, 161440. [CrossRef]
2. Prince, S.; Avimanyu, D.; Gary, W.; Courtney, Y. Recovery of metal values from copper slag and reuse of residual secondary slag. *Waste Manag.* **2017**, *70*, 272–281.
3. Wenhuan, L.; Hui, L.; Huimei, Z.; Pinjing, X. Properties of a Steel Slag–Permeable Asphalt Mixture and the Reaction of the Steel Slag–Asphalt Interface. *Materials* **2019**, *12*, 3603.
4. Hao, S.; Luo, G.P.; Lu, Y.Y.; An, S.L.; Chai, Y.F.; Song, W. Effect of High Temperature Reconstruction and Modification on Phase Composition and Structure of Steel Slag. *Minerals* **2022**, *13*, 67. [CrossRef]
5. Islam, Z.; Tran, Q.T.; Koizumi, S.; Kato, F.; Ito, K.; Araki, K.S.; Kubo, M. Effect of Steel Slag on Soil Fertility and Plant Growth. *J. Agric. Chem. Environ.* **2022**, *11*, 209–221. [CrossRef]
6. Liu, Z.y.; Ni, W.; Li, Y.; Ba, H.j.; Li, N.; Ju, Y.J.; Zhao, B.; Jia, G.L.; Hu, W.T. The mechanism of hydration reaction of granulated blast furnace slag-steel slag-refining slag-desulfurization gypsum-based clinker-free cementitious materials. *J. Build. Eng.* **2021**, *44*, 103289. [CrossRef]
7. She, J. Experimental Study on the Removal of Phosphate from Wastewater by Modified Steel Slag. Ph.D. Thesis, Wuhan University of Technology, Wuhan, China, 2007.
8. Xing, C.; Yao, N.; Zhang, L.W. Mechanistic study on the effect of SiO_2 content on the self-pulverization of steel slag. *Miner. Compr. Util.* **2016**, *06*, 89–91.
9. Cárdenas, C.; Mácová, P.; Gómez, M.y.; Zárybnická, L.c.; Ševčík, R.; Viani, A. Formation, Properties, and Microstructure of a New Steel Slag–Based Phosphate Cement. *J. Mater. Civ. Eng.* **2021**, *33*, 3958. [CrossRef]
10. Haiyan, Y.; Xiaolin, P.; Kaiwei, D.; Yan, W. Effect of P addition on mineral transition of CaO-Al_2O_3-SiO_2 system during high-temperature sintering. *Trans. Nonferrous Met. Soc. China* **2019**, *29*, 650–656.
11. Xie, D.W. Study on the Influence of Steel Slag Composition on Its Self-Pulverization Process. Ph.D. Thesis, Anhui University of Technology, Ma'anshan, China, 2015.
12. Lee, J.C.; Park, S.W.; Kim, H.S.; Alam, T.; Lee, S.Y. Oxidation Enhancement of Gaseous Elemental Mercury Using Waste Steel Slag under Various Experimental Conditions. *Sustainability* **2023**, *15*, 1406. [CrossRef]
13. Du, C.M.; Gao, X.; Ueda, S.G.; Kitamura, S.Y. Effect of Fe^{2+}/T.Fe Ratio on the Dissolution Behavior of P from Steelmaking Slag with High P_2O_5 Content. *J. Sustain. Metall.* **2018**, *4*, 443–454. [CrossRef]
14. Wang, J.J.; Zhang, L.F.; Cheng, G.R.; Qiang, R.Y. Dynamic mass variation and multiphase interaction among steel, slag, lining refractory and nonmetallic inclusions: Laboratory experiments and mathematical prediction. *Int. J. Miner. Metall. Mater.* **2021**, *28*, 1298–1308. [CrossRef]
15. Liu, P.J.; Liu, Z.G.; Chu, M.S.; Tang, J.; Gao, L.H.; Yan, R.J. Green and efficient utilization of stainless steel dust by direct reduction and self-pulverization. *J. Hazard. Mater.* **2021**, *413*, 125403. [CrossRef]
16. Huang, D.Y. Research on Carbon Thermal Reduction Self-Powdering of Converter Steel Slag. Ph.D. Thesis, Anhui University of Technology, Ma'anshan, China, 2016.
17. Han, Y.L.; Yang, X.B.; Qian, F.P.; Hu, Y.M. NO Removal on Activated Coke Mixed with Steel Slag and Coke Powder. *Chem. Eng. Technol.* **2021**, *44*, 140. [CrossRef]
18. Xie, D.W.; Wang, Y.; Jiang, L.; Wang, J.; Gao, W.; Dong, Y.C. Feasibility study of self-pulverization of converter steel slag. *J. Anhui Univ. Technol. (Nat. Sci. Ed.)* **2016**, *33*, 105–109.
19. Peng, W.F.; Yang, N.; Yang, M.Y.; Li, S. Study on the melting temperature of CaO-SiO_2-Al_2O_3-TiO_2 system. *World Nonferrous Met.* **2020**, *21*, 210–212.
20. Guo, Y.C.; Zheng, H.Y.; Hu, X.G.; Shen, F.M. Prediction model of Al_2O_3 activity in CaO-SiO_2-MgO-Al_2O_3 quaternary slag system. *J. Northeast. Univ. (Nat. Sci. Ed.)* **2021**, *42*, 652–657.
21. Pang, Z.D.; Lv, X.W.; Yan, Z.M.; Bai, C.K.; Xie, H.N.; Pan, C. Super high TiO_2 blast furnace slag viscosity and meltability temperature. *Steel* **2020**, *55*, 181–186.
22. Liu, Y.; Zhang, C.X. Current status and development trend of comprehensive utilization of iron and steel slag. *Miner. Compr. Util.* **2019**, *2*, 21–25.

23. Yan, Z.W.; Deng, Z.Y.; Zhu, M.Y. Effect of $CaCl_2$ Addition on the Viscosity of CaO–SiO_2–FeO_x Steelmaking Slag System. *Metall. Mater. Trans.* **2021**, *52*, 2474–2483. [CrossRef]
24. Cheng, Z.R.; Gao, J.T.; Wang, Z.W.; Guo, Z.C. Effect of P content on solid solution behavior of CaO-SiO_2-P_2O_5-Fe_tO-MgO slag system P and supergravity separation of nC_2S-C_3P. *Jiangxi Metall.* **2021**, *41*, 25–30.

Disclaimer/Publisher's Note: The statements, opinions and data contained in all publications are solely those of the individual author(s) and contributor(s) and not of MDPI and/or the editor(s). MDPI and/or the editor(s) disclaim responsibility for any injury to people or property resulting from any ideas, methods, instructions or products referred to in the content.